

**On the relation between index  
cycles of the atmosphere  
circulation and spatial  
spectrum of the kinetic energy  
in the model of the general  
circulation of the atmosphere**

G.I. Marchuk, V.P. Dymnikov and  
V.N. Lykossov

Research Department

May 1981

The simulation of index cycles of the atmospheric circulation is a very important and complex problem (especially for long term weather forecasts). Beginning from pioneer publications by Rossby (1939) and Blinova (1947), many articles considering this problem have been published. We do not give here the full description of all investigations on this problem; we should like to point out only those works which have a direct relationship with the subject of this paper.

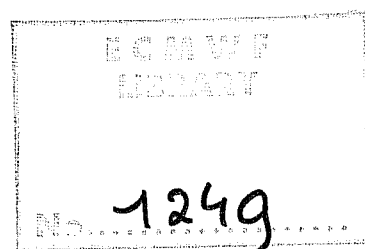
Monin (1956) has analyzed a time spectrum of oscillations of zonal circulation of the atmosphere and he has found 15 and 24 day periodicities of index cycles oscillations. Monin has expelled a basic component of annual variations of index cycles of the circulation. The annual oscillation of index has been analyzed by Marchuk (1958).

Miller (1974) has used a spectral analysis of selected components of the atmospheric cycle of the energy and he has shown that there is a relative maximum at 14-16 day periods in corresponding distributions of energy (both kinetic and available potential) and its conversions as well.

Webster and Keller (1975) and McGuirk and Reiter (1976) have investigated approximately 24 day oscillations of energy components and of zonal index, which have been introduced as a relation of eddy kinetic energy to zonal kinetic energy.

It should be noted that in all the above mentioned papers, the measure of circulation index is different (wind velocity, energy components, etc.) but these quantities have been averaged over large enough areas (up to the hemisphere). We should also like to mention that, in all these works, observation data from different sources have been used.

We should like to point out especially the paper by Kurbatkin and Lenskinov (1968) where an attempt to simulate a cycle index has been made. In this work, it was shown that in the presence of especially chosen forcing ("climatic source") in a barotropic model of the atmosphere, there might be auto oscillations with periods of 14 or 24 days.



A difficulty of the problem is, that in order to reproduce nonlinear oscillations of such a system as the atmosphere, we have to reproduce not only the generation level of eddy kinetic energy (which is determined by adequate description of the thermodynamics of the atmosphere) but also the redistribution of this energy in spatial spectrum, which is especially important.

Let us assume that a basic generation of eddy kinetic energy has occurred in the middle latitudes in spectral range of synoptic scales by means of realization of the baroclinic instability. The atmosphere is approximately barotropic and geostrophic and, therefore, in this case, there must be an energy transport into side of more smaller wavenumbers. At the same time, there is an enstrophy transport into side of more larger wavenumbers, giving well known "-3 law" in the spectral distribution of the kinetic energy.

If a model of the general circulation of the atmosphere is constructed so that it has (for example, in barotropic case) the laws of conservation of energy and enstrophy at the same time (of course, we bear in mind the finite difference approximations in finite dimension space to these laws), it seems to us that laws of spectral distribution of energy have to be got automatically and non linear oscillations (its amplitudes and phases) will be determined mainly by levels of generation and dissipation of the energy. (We bear in mind only baroclinic source of the energy when eddy transferring heat to pole decrease a level of available potential energy and, therefore, take away the source itself).

In the opposite case, we have to think not only about levels of generation and dissipation of energy but on construction of corresponding gradients in spectral distribution of energy as well. Of course, we assume that mean profile of zonal component of velocity has been reproduced sufficiently.

In order to check the assumptions described above, numerical experiments with a model of the general circulation of the atmosphere developed in the Computer Centre of the Siberian Branch of the USSR Academy of Sciences have been carried out. In this article, a brief description of the model and problems has been given and some results of numerical calculations have been discussed.

# 1. DESCRIPTION OF THE MODEL

## 1.1 Hydrodynamic equations

If one takes the pressure normalized to its value at the Earth's surface to be the vertical coordinate and used the quasistatic approximation, the hydrodynamic equations can be written in spherical coordinates as follows:

$$\frac{du}{dt} + \left(f + \frac{u}{a} \operatorname{tg} \phi\right)v + \frac{1}{\operatorname{acos} \phi} \left(\frac{\partial \phi}{\partial \lambda} + \frac{RT}{p_s} \frac{\partial p_s}{\partial \lambda}\right) = F_u \quad (1a)$$

$$\frac{dv}{dt} - \left(f + \frac{u}{a} \operatorname{tg} \phi\right)u + \frac{1}{a} \left(\frac{\partial \phi}{\partial \phi} + \frac{RT}{p_s} \frac{\partial p_s}{\partial \phi}\right) = F_v \quad (1b)$$

$$\frac{\partial p_s}{\partial t} + \frac{1}{\operatorname{acos} \phi} \left(\frac{\partial p_s u}{\partial \lambda} + \frac{\partial p_s v \operatorname{cos} \phi}{\partial \phi}\right) + \frac{\partial p_s \sigma}{\partial \sigma} = 0 \quad (1c)$$

$$\frac{dT}{dt} - \frac{RT}{c_p \sigma p_s} \left[p_s \sigma + \sigma \left(\frac{\partial p_s}{\partial t} + \frac{u}{\operatorname{acos} \phi} \frac{\partial p_s}{\partial \lambda} + \frac{v}{a} \frac{\partial p_s}{\partial \phi}\right)\right] = F_T + \epsilon \quad (1d)$$

$$\frac{dq}{dt} = F_q - (C-E) \quad (1e)$$

$$\frac{\partial \phi}{\partial \sigma} = - \frac{RT}{\sigma} \quad (1f)$$

where 
$$\frac{d}{dt} = \frac{\partial}{\partial t} + \frac{u}{\operatorname{acos} \phi} \frac{\partial}{\partial \lambda} + \frac{v}{a} \frac{\partial}{\partial \phi} + \sigma \frac{\partial}{\partial \sigma}$$

Here the following notations are used:

- $t$  = time
- $\lambda$  = longitude
- $\phi$  = latitude
- $\sigma$  =  $p/p_s$  ( $p$  being pressure and  $p_s$  - its value at the Earth's surface) = the vertical coordinate.
- $u, v, \dot{\sigma}$  = wind components in  $\lambda, \phi$  and  $\sigma$  respectively.
- $\Phi$  =  $gz$  ( $g$  being acceleration due to gravity,  $z$  - altitude at sea level) = geopotential of constant  $\sigma$ - surface
- $T$  = absolute temperature
- $q$  = specific humidity
- $f$  =  $2\Omega \sin \phi$  ( $\Omega$  being the angular velocity of the Earth), the Coriolis parameter
- $a$  = mean radius of the Earth
- $R$  = gas constant of air
- $c_p$  = specific heat of air at constant pressure
- $F_u, F_v$  = rates of change of momentum caused by Reynolds stresses
- $F_t, F_q$  = rates of change of temperature and specific humidity caused by small-scale diffusion
- $\epsilon$  = diabatic heating rate ( $\epsilon = \epsilon_r + \epsilon_f$ , where  $\epsilon_r$  and  $\epsilon_f$  are radiative and latent heating rates, respectively).
- $C$  = term describing the condensation process.
- $E$  = evaporation.

The solution is assumed to be periodic, which is also taken as the boundary condition for (1) in  $\lambda$  and  $\phi$ . The underlying surface is also taken to be a solid body corresponding to the  $\sigma$ -coordinate surface  $\sigma = 1$ . The corresponding kinematic condition is

$$\dot{\sigma} = 0 \quad \text{at } \sigma = 1 \quad (2)$$

A similar condition is on the upper boundary of the atmosphere

$$(p = 0) \quad \dot{\sigma} = 0 \quad \text{at } \sigma = 0 \quad (3)$$

If  $\sigma = 1$ , then in addition to (2), we have the geopotential distribution

$$\phi = gZ_s \equiv \phi_s \text{ at } \sigma = 1 \quad (4)$$

where  $Z_s$  is elevation of the Earth's surface above sea level.

## 2. PARAMETERIZATION OF SUB-GRID SCALE PROCESSES

### 2.1 Interaction of the atmosphere and the underlying surface

We define the fluxes of momentum module ( $|\vec{\tau}_s|$ ), heat ( $H_s$ ) and moisture ( $E_s$ ) at the Earth's surface by

$$|\vec{\tau}_s| = -\rho_h |\vec{V}_h|^2 C_u \quad (5a)$$

$$H_s = -C_p \rho_h |\vec{V}_h| (T_h - T_s) C_T \quad (5b)$$

$$E_s = -r \rho_h |\vec{V}_h| (q_h - q_{\max}(p_s, T_s)) C_T \quad (5c)$$

where  $\rho$  is air density,  $\vec{v}$  the horizontal wind velocity,  $q_{\max}$  the saturated value of specific humidity,  $r$  the relative humidity, and  $C_u$ ,  $C_T$  the friction and heat exchange coefficients, respectively. Subscript h refers to values at the upper boundary of the surface sublayer of constant fluxes, and subscript s refers to functions defined at  $\sigma = 1$ .

Along with the surface sublayer of constant fluxes, above lying well mixed layer is considered. We assume that its upper boundary has the same altitude at the sea level as the nearest to the Earth's surface the calculation level.

Below subscript KL refers to values at this level. We assume also that, in mixed layer, a module of the velocity vector  $\vec{V}$  is constant along the height and therefore  $|\vec{V}_h| = |\vec{V}_{KL}|$  (with the constraint  $|\vec{V}_k| \geq 1$  m/sec).

The wind velocity vector is different from the surface stress vector direction at the upper level of the mixed layer. The angle between those two vectors is chosen as  $20^\circ$  above the ocean,  $30^\circ$  above the land and  $10^\circ$  above ice (outside the tropical area  $|\phi| \geq 20^\circ$ ).

In the tropical area ( $|\phi| < 20^\circ$ ) this angle is equal to  $0^\circ$

To calculate the temperature  $T_h$  and specific humidity  $q_h$ , it is assumed that the flux of pseudo-potential temperature

$$\theta = \left(\frac{1000 \text{ mb}}{p}\right)^{R/C_p} \left(T + \frac{L}{C_p} q\right)$$

(L is the latent heat of evaporation)

in the surface sublayer is equal to its flux outside that layer

$$-\rho_h |\vec{V}_h| (\theta_h - \theta_s) C_T = -\rho_H K_V \frac{\theta_{KL} - \theta_h}{z_{KL} - z_h} \quad (6)$$

with the relation

$$q_h = r q_{\max}(p_s, T_h)$$

In (6)  $K_V$  is the vertical diffusion coefficient (it is assumed that  $K_V = \alpha |\vec{V}_h|$ ,  $\alpha \sim 1 \text{ m}$ ). If the mixed layer is dry, or moist unstable, algorithm of the convective adjustment has been used. It is assumed that total amount of condensed moisture in the mixed layer is evaporating immediately and therefore it does not give precipitation.

The coefficients  $C_u$  and  $C_T$  are chosen as follows. In the case of the neutral stratification ( $\Delta T = T_h - T_s \approx 0$ )

$C_u = C_u^N$ ,  $C_T = C_T^N$ , where above land and ice

$$C_u^N = C_T^N = 0.002 (1 + 3z_s^*/z_s^*) \quad (7)$$

(the parameter  $z_s^*$  has the dimension of length and is equal to 5000 m).

Above ocean (Wu, 1969)

$$C_u^N = \begin{cases} 0.0005 \sqrt{|\vec{V}_h|} & \text{if } |\vec{V}_h| \leq 15 \text{ m/sec} \\ 0.0026 & \text{if } |\vec{V}_h| \geq 15 \text{ m/sec} \end{cases} \quad (8)$$

$$C_T^N = C_u^N / \begin{cases} 1.2 & \text{if } |\vec{V}_h| < 5 \text{ m/sec} \\ 1 & \text{if } 5 \text{ m/sec} \leq |\vec{V}_h| \leq 10 \text{ m/sec} \\ 0.7 & \text{if } |\vec{V}_h| > 10 \text{ m/sec} \end{cases} \quad (9)$$

In the case of stable or unstable stratification ( $\Delta T \neq 0$ )

$$C_u = C_u^N f_T(Ri), \quad C_T = C_T^N f_T(Ri) \quad (10)$$

where  $Ri$  is the bulk Richardson number

$$Ri = - \frac{\frac{g}{\theta_h} (z_h - z_s) \Delta T}{|\vec{v}_h|^2}$$

In the present version of the model, a value of  $(z_h - z_s)$  is chosen equal to 70 m, the function  $f_T$  is assumed as follows (Arakawa, 1972).

$$f_T(Ri) = \begin{cases} 1 + 3 Ri & \text{if } Ri < 0 \text{ (the stable stratification)} \\ 1 + 0.65 Ri^{1/2} & \text{if } Ri > 0 \text{ (the unstable stratification)} \end{cases} \quad (11)$$

The temperature of the ocean surface is assumed to be either a known function of latitude and longitude or it is found from the integral model of the ocean active layer (Kitaygorodskiy and Miropolskiy, 1970):

$$\frac{\partial T_s}{\partial t} = \frac{B_s - B_\eta}{C_{pW} \rho_w \eta} \quad (12a)$$

$$\frac{\partial \eta}{\partial t} = \frac{1}{C_{pW} \rho_w \alpha_w (T_s - T_H)} \left[ B_\eta - (1 - \alpha_w) (H - \eta) \frac{B_s - B_\eta}{\eta} \right] \quad (12b)$$

$$B_\eta = - B_s + \frac{2 C_{pW} \rho_w C_w (1 - \delta_w) u_*^3}{g \gamma \eta} \quad (12c)$$

$$B_s = (1 - \alpha_s) S_g + F_g - \sigma_{SB} T_s^4 - H_s - LE_s \quad (12d)$$

Here  $T_s$  and  $T_H$  are the temperatures of the water at the surface and at depth  $H$  (in the model  $H = 300$  m):



$\eta$  is the depth of the mixed layer;  $B_s$  and  $B_\eta$  are heat fluxes at the surface of the ocean and at depth  $\eta$  ( $\eta < H$ );  $C_{pw}$  and  $\rho_w$  are the specific heat and density of sea water;  $\gamma$  is the sea water buoyancy parameter;  $\alpha_w$ ,  $C_w$  and  $\delta_w$  are dimensionless constants equal to 0.7, 30 and 0.98, respectively;  $\sigma_{SB}$  is the Stefan-Boltzmann constant;  $\alpha_s$  is the albedo of the underlying surface;  $S_g$  and  $F_g$  are the total fluxes of solar and long-wave radiation at the Earth's surface; and  $u_*$  is the friction velocity equal to  $\sqrt{|\tau_s|/\rho_w}$ .

To calculate the temperature of the ground and the ice, the heat balance equation has been employed

$$H_s + LE_s + \sigma_{SB} T_s^4 + B_s = (1 - \alpha_s) S_g + F_g \quad (13)$$

For the ground, it is assumed that  $B_s = 0$ ; in the case of sea ice, the flux is calculated by the formula  $B_s = \lambda_i (T_s - T_H)/H$ , where  $H$  is the thickness of the ice,  $\lambda_i$  is the coefficient of heat conductivity, and  $T_H$  is the freezing temperature of sea water. In model  $T_H = 271.5$  K,  $H = 3$  m, and  $\lambda_i = 0.005$  cal/cm<sup>2</sup> sec deg. The value of  $\alpha_s$  is given as follows:

$$\alpha_s = \begin{cases} 0.1 & \text{for the surface of the ocean} \\ 0.2 (1+2S) & \text{for the surface of the ground} \\ 0.6 & \text{for the ice} \end{cases} \quad (14)$$

with the constraints  $\alpha_s \leq 0.6$ .

In (14)  $S$  is the water equivalent depth of snow. If the temperature of the underlying surface  $T_s$  in the regions covered with ice or snow appears as a result of calculation by formula (13) to be higher than the melting temperature  $T_m = 273.2^\circ\text{K}$ , we let  $T_s = T_m$ , and calculate the rate of snow (or ice) melting as

$$M_{sn} = \begin{cases} E_x/L_m, & \text{if } E_x > 0 \\ 0, & \text{if } E_x \leq 0 \end{cases} \quad (15a)$$

$$E_x = [ (1 - \alpha_s) S_g + F_g - \sigma_{SB} T_s^4 - LE_s - H_s ]_{T_s = T_m} \quad (15b)$$

where  $L_m$  is the latent heat of melting.

The depth of snow is calculated by

$$\frac{\partial S}{\partial t} = \delta_{sn} - E_s - M_{sn} \quad (16)$$

where  $\delta_{sn}$  is the rate of snowfall.

The relative humidity of air  $r$  is taken to be 1 above oceans and regions covered with snow or ice; in other regions of the earth  $r$  is defined by

$$r = \begin{cases} W/W_{cr} & \text{if } W \leq W_{cr} \\ 1 & \text{if } W > W_{cr} \end{cases} \quad (17)$$

where  $W$  is the humidity of the ground layer up to the depth = 1 m,  $W_{cr} = 0.75 W_f$ , and  $W_f$  is the moisture capacity of the ground,  $W_f = 15$  cm. If the amount of precipitation exceeds  $W_f$ , the moisture excess is assumed to flow either to other regions of the ground or to the ocean:

$$\frac{\partial W}{\partial t} = \delta - E_s, \text{ if } W < W_f \quad (18a)$$

$$\frac{\partial W}{\partial t} = 0, \text{ if } W = W_f, \delta > E_{s,max} \quad (18b)$$

Here  $\delta$  is precipitation intensity and  $E_{s,max}$  is the flux of moisture under saturation. The moisture content of snow is assumed to be zero. To calculate the moisture of the ground under snow cover, we employ the relations

$$\frac{\partial W}{\partial t} = M_{sn} + \delta, \text{ if } W < W_f \quad (19a)$$

$$\frac{\partial W}{\partial t} = 0, \text{ if } W \geq W_f \quad (19b)$$

## 2.2 Small-scale diffusion

The rates of change of momentum, temperature and moisture caused by small-scale diffusion consist of two parts,  $F = F^H + F^V$ , where subscripts H and V denote the contributions of horizontal diffusion and vertical mixing, respectively. The vertical diffusion and its parameterization in model have been described above.

The horizontal turbulent small-scale diffusion must not affect the total angular momentum of the system. This imposes certain constraints on finite-difference approximations of diffusive terms satisfying dissipative conditions and the conservation of global angular momentum if these terms are represented as

$$F_u^H = \frac{1}{a^2 \cos^2 \phi p_s} \left[ \frac{\partial}{\partial \lambda} p_s K_H \frac{\partial u}{\partial \lambda} + \frac{\partial}{\partial \phi} p_s K_H \cos^3 \phi \frac{\partial \frac{u}{\cos \phi}}{\partial \phi} \right] \quad (20a)$$

$$F_s^H = \frac{1}{a^2 \cos^2 \phi p_s} \left[ \frac{\partial}{\partial \lambda} p_s K_H \frac{\partial s}{\partial \lambda} + \cos \phi \frac{\partial}{\partial \phi} p_s K_H \cos \phi \frac{\partial s}{\partial \phi} \right] \quad (20b)$$

where  $S = v, T, q$ . In (20)  $K_H$  is the horizontal diffusion coefficient, which has been chosen as follows (Smagorinsky, 1963):

$$K_M = \mu \left[ K_H^0 + l^2 \sqrt{D_T^2 + D_S^2} \right] \quad (21)$$

where

$$D_T = \frac{1}{a \cos \phi} \frac{\partial u}{\partial \lambda} - \frac{\cos \phi}{a} \frac{\partial}{\partial \phi} \left( \frac{v}{\cos \phi} \right) \quad (22a)$$

$$D_S = \frac{1}{a \cos \phi} \frac{\partial v}{\partial \lambda} + \frac{\cos \phi}{a} \frac{\partial}{\partial \phi} \left( \frac{u}{\cos \phi} \right) \quad (22b)$$

$$l^2 = 0.08 a^2 (\cos^2 \phi \Delta \lambda^2 + \Delta \phi^2) \quad (22c)$$

( $\Delta \lambda$  and  $\Delta \phi$  are parameters of the grid domain)

$$K_H^0 = \text{const} = 50000 \text{ m}^2/\text{sec} \quad (22d)$$

$\mu$  is a parameter which gives the possibility of changing the model dissipation level in numerical experiments.

### 2.3 Large-scale condensation

The large-scale condensation process is described by

$$\frac{\partial T}{\partial t} = \frac{L}{c_p} (C - E) \quad (23a)$$

$$\frac{\partial q}{\partial t} = - (C - E) \quad (23b)$$

This system of equations is solved using the following equations:

- a. The process of evaporation in clouds may be neglected.
- b. All condensed moisture falls onto the surface of the earth.
- c. The specific humidity in clouds is equal to the saturated specific humidity,  $q = q_{\max}$ .
- d. Clouds occurring during the calculation fill the whole computational cell.

The difference approximation of this problem for time step  $n$  is

$$\frac{L}{c_p} (q^{n+1} - q^n) = (T^{n+1} - T^n) \quad (24a)$$

$$q^{n+1} = q_{\max} (T^{n+1}), \quad (24b)$$

which is solved by an iterative method.

### 2.4 Parameterization of the amount of nonconvective clouds and of dry and moist convection

To calculate the amount of nonconvective clouds in the model, the linear relations between the cloud amount ( $C$ ) and relative humidity ( $r$ ) have been used (Smagorinsky, 1960):

$$C = \alpha r + \beta \quad (25)$$

Cloudiness is assumed to be of three layers: the upper layer is between  $p = 300$  mb and  $p = 550$  mb, the middle layer is between  $p = 550$  mb and  $p = 700$  mb, and the lower layer is between  $p = 700$  mb and  $p = 850$  mb. For the upper layer,  $\alpha = 1.73$ ,  $\beta = 0.43$ , for the middle layer  $\alpha = 2$ ,  $\beta = 0.7$  and for the lower level  $\alpha = 3.33$ ,  $\beta = -2$ .

Algorithms of the parameterization of dry and moist convection are as follows. Dry convection arises if

$$\frac{T_{k+1} - T_k}{P_{k+1} - P_k} > \gamma_a \frac{RT_{k+\frac{1}{2}}}{gP_{k+\frac{1}{2}}} \quad (26)$$

where

$$T_{k+\frac{1}{2}} = \frac{T_k + T_{k+1}}{2}$$

$\gamma_a$  is dry adiabatic lapse rate, and  $k$  the number of the level. The equations of dry convective adjustment are

$$\frac{\tilde{T}_{k+1} - \tilde{T}_k}{P_{k+1} - P_k} = \frac{\gamma_a RT_{k+\frac{1}{2}}}{gP_{k+\frac{1}{2}}} \quad (27a)$$

$$(\tilde{T}_{k+1} - T_{k+1}) + (\tilde{T}_k - T_k) = 0 \quad (27b)$$

(Here and below the wave over a symbol refers to redefined values).

The condition of moist convection is expressed by

$$\frac{T_{k+1} - T_k}{P_{k+1} - P_k} > \frac{\gamma_c RT_{k+\frac{1}{2}}}{gP_{k+\frac{1}{2}}} \quad (28a)$$

$$r_k > r_{cr}, r_{k+1} > r_{cr} \quad (28b)$$

where

$$r_k = \frac{q_k}{q_{\max}(p_k, T_k)}, \quad r_{cr} = 0.7 \quad (29a)$$

$$\gamma_c = \gamma_a \frac{1 - r_k}{1 - r_{cr}} + \gamma_{ca} \frac{r - r_{cr}}{1 - r_{cr}} \quad (29b)$$

$$\tau = \frac{r_k + r_{k+1}}{2} \quad (29c)$$

and  $\gamma_{ba}$  is the moist adiabatic lapse rate.

The equations of moist convective adjustment are of the form

$$(\tilde{q}_{k+1} - q_{k+1}) + (\tilde{q}_k - q_k) + m = 0 \quad (30a)$$

$$(\tilde{T}_{k+1} - T_{k+1}) + (\tilde{T}_k - T_k) - \frac{L}{C_p} m = 0 \quad (30b)$$

$$\tilde{q}_k = r_{cr} q_{\max}(p_k, \tilde{T}_k), \quad \tilde{q}_{k+1} = r_{cr} q_{\max}(p_{k+1}, \tilde{T}_{k+1}) \quad (30c)$$

$$\frac{\tilde{T}_{k+1} - \tilde{T}_k}{p_{k+1} - p_k} = \gamma_c \frac{\tilde{R}T_{k+\frac{1}{2}}}{g p_{k+\frac{1}{2}}} \quad (30d)$$

In (30)  $m$  is the total amount of condensed moisture.

## 2.5 Radiation

Long-wave cooling of atmosphere layers is calculated by the well-known formulae:

$$F_p^\uparrow = B_p + \int_{B_p}^B \tau(u_p^* - u^*) dB + (B_{gr} - B_g) \tau(u_p^*) \quad (31a)$$

$$F_p^\downarrow = B_p - \int_{B_1}^B \tau(u^* - u_p^*) dB - (B_1 - B_c) \tau(u_1^* - u_p^*) \quad (31b)$$

where  $B_{\alpha} = \sigma_{SB} T_{\alpha}^4$  is black-body emission;  $\tau$  the integral transmission function;  $u_p^*$  the effective amount of absorbing gas from the underlying surface up to level  $p$ ;  $B_{gr}$  and  $B_g$  are introduced to denote the radiation of the underlying surface and of the atmosphere above it, respectively, allowing for a possible jump in temperature;  $B_c$  and  $B_1$  play a similar role for downward radiation at the upper boundary of the atmosphere.

Integrals of the type

$$\int_{B_p}^{B_g} \tau(u_p^* - u^*) dB$$

over layers nonadjacent to level  $p$  are calculated by the ordinary trapezoidal formula, and the three-point method of Gauss is employed in the layer of the largest change of the integrand (level  $p$  being one of the boundaries of the layer). This ensures at least one correct symbol following the comma in the value of the heating rate.

In the short-wave region of the spectrum, fluxes are determined separately for a cloudy and cloudless atmosphere. In the region of wavelengths, less than  $0.9\mu$  in a cloudless atmosphere, absorption by ozone and Rayleigh scattering are considered (Lacis and Hansen, 1974). In the case of a cloudy sky, absorption by ozone in the atmosphere above clouds and dissipation in clouds are taken into consideration, whereas Rayleigh scattering is neglected. In the region of wavelengths greater than  $0.9\mu$ , Katayama's method has been used (Katayama, 1972). In addition, the model contains an algorithm of the method of layer doubling from Lacis and Hansen.

### 3. NUMERICAL REALIZATION OF THE MODEL

A grid domain is selected, on which the unknown functions are defined. In the vertical, the analog of vertical velocity  $\dot{\sigma}$  is shifted half a step with respect to the other unknown functions. The horizontal grid is so constructed that the components of the velocity vector  $u, v$  are shifted half a step in  $\phi$  and  $\lambda$  with respect to other unknown functions (the grid point for  $u$  and  $v$  is not a polar point).

The system of equations (1) is reduced to a so-called symmetric form by transforming the dependent variables  $(u, v, T, q)$  into  $(u \sqrt{p_s}, v \sqrt{p_s}, T \sqrt{p_s}, q \sqrt{p_s})$ , where  $p_s$  is the surface pressure. The main purpose of this symmetrization is to obtain relatively simple and absolutely stable difference schemes for the

solution of multidimensional equations for the transfer of substances along trajectories and also for satisfactory finite difference approximations to the integral laws of conservation. The problem is solved by the splitting-up method (Marchuk, 1974). At every time step ( $\Delta t$ ) the solutions of the equations of transfer, diffusion and adaptation are considered separately.

### 3.1 Solution of transfer equations

If  $\psi$  is any component of the vector  $(u \sqrt{p_s}, v \sqrt{p_s}, T \sqrt{p_s}, q \sqrt{p_s})$  and  $\tilde{v} = v \cos \phi$ , one can write the transfer equation for  $\psi$ , as follows:

$$\frac{\partial \psi}{\partial t} + \frac{1}{a \cos \phi} \left( \frac{1}{2} u \frac{\partial \psi}{\partial \lambda} + \frac{1}{2} \frac{\partial u \psi}{\partial \lambda} + \frac{1}{2} \tilde{v} \frac{\partial \psi}{\partial \phi} + \frac{1}{2} \frac{\partial v \psi}{\partial \phi} \right) + \frac{1}{2} \dot{\sigma} \frac{\partial \psi}{\partial \sigma} + \frac{1}{2} \frac{\partial \dot{\sigma} \psi}{\partial \sigma} = 0 \quad (32)$$

In (32) a value of the quantity  $(\psi, \psi)$ , which equals

$$\int_0^1 \int_{-\pi/2}^{\pi/2} \int_0^{2\pi} \psi^2 a^2 \cos \phi \, d\lambda \, d\psi \, d\sigma$$

has been retained. This means that a spatial operator in (32) has a skew-symmetric form. Also the symmetrization of the transfer equations gives a skew-symmetric form for one-dimensional equations.

Applying (32), the method of component-by-component splitting and the Crank-Nicholson scheme, we shall have a system of one-dimensional equations:

$$\frac{\psi^{n+1/3} - \psi^n}{\Delta t} + A_1 \frac{\psi^{n+1/3} + \psi^n}{2} = 0 \quad (33a)$$

$$\frac{\psi^{n+2/3} - \psi^{n+1/3}}{\Delta t} + A_2 \frac{\psi^{n+2/3} + \psi^{n+1/3}}{2} = 0 \quad (33b)$$

$$\frac{\psi^{n+1} - \psi^{n+2/3}}{\Delta t} + A_3 \frac{\psi^{n+1} + \psi^{n+2/3}}{2} = 0 \quad (33c)$$

where  $A_1$ ,  $A_2$  and  $A_3$  are difference analogs of transfer operators on  $\lambda$ ,  $\phi$  and  $\sigma$ , respectively, which possess the property of skew-symmetry  $(A_1 \psi, \psi) = 0$ . A dot product in finite-dimensional space is defined, as follows:



$$(\psi, \xi) = \sum_i \sum_j \sum_k \psi_{ijk} \zeta_{ijk} a^2 \cos \phi_j \Delta \lambda \Delta \phi \Delta \sigma_k$$

where  $\Delta \lambda$ ,  $\Delta \phi$ , and  $\Delta \phi_k$  are the parameters of the finite-difference grid. A construction of finite-difference analogs of symmetrized operators is not difficult; a skew-symmetric property of  $A_i$  automatically gives a relation

$$(\psi^{n+1}, \psi^{n+1}) = (\psi^n, \psi^n)$$

Transfer in  $\lambda$  (along circles of latitude) is carried out by the cyclic factorization method and is identical for all unknown functions (the difference being in defining "transferring" velocities). The algorithm of transfer along  $\sigma$  is also identical for all unknown functions (scalar factorization). It is more difficult to treat the transfer in  $\phi$  (along meridians).

In the present model, the method of formation of cyclically closed circles of meridians shifted by  $180^\circ$  with respect to one another has been used. The components of vector quantities change their sign to an opposite one when passing through the pole, while scalar values do not change their sign. Since the polar point is not a point of definition of  $u$  and  $v$ , there is no problem in transferring the velocity vector components along such closed circles (the transfer is carried out by cyclic factorization). Here skew-symmetry of the operator guarantees conservation of quadratic values.

### 3.2 Solution of diffusion equations

To solve the diffusion equations, the method of spatial component-by-component splitting and the Crank-Nicholson scheme in time has been used. It is very simple to construct the finite-difference analogs of corresponding operators, which would have a property of dissipativity. To solve a system of finite-difference equations, similar methods as described above have been used.

### 3.3 Solution of adaptation equations

The system of hydrothermodynamic equations at the stage of adaptation can be written, as follows:

$$\frac{\partial \sqrt{p_s} u}{\partial t} - \left( f + \frac{utg\phi}{a} \right) \sqrt{p_s} v + \frac{\sqrt{p_s}}{a \cos\phi} \left( \frac{\partial \phi}{\partial \lambda} + RT \frac{\partial \ln p_s}{\partial \lambda} \right) = 0 \quad (34a)$$

$$\frac{\partial \sqrt{p_s} v}{\partial t} + \left( f + \frac{utg\phi}{a} \right) \sqrt{p_s} u + \frac{\sqrt{p_s}}{a} \left( \frac{\partial \phi}{\partial \phi} + RT \frac{\partial \ln p_s}{\partial \phi} \right) = 0 \quad (34b)$$

$$\frac{\partial \sqrt{p_s} T}{\partial t} - \frac{RT}{c_p \sqrt{p_s}} \left( \frac{\partial p_s}{\partial t} + \frac{u}{a \cos\phi} \frac{\partial p_s}{\partial \lambda} + \frac{v}{a} \frac{\partial p_s}{\partial \phi} \right) - \frac{RT \sqrt{p_s} \dot{\sigma}}{c_p \sigma} = 0 \quad (34c)$$

$$\frac{\partial p_s}{\partial t} + \frac{1}{a \cos\phi} \left( \frac{\partial p_s u}{\partial \lambda} + \frac{\partial p_s \cos\phi v}{\partial \phi} \right) + \frac{\partial}{\partial \sigma} p_s \dot{\sigma} = 0 \quad (34d)$$

$$\frac{\partial \phi}{\partial \sigma} = - \frac{RT}{\sigma} \quad (34e)$$

During this stage, the second-order accuracy scheme for the approximation of the equations in space, and the Crank-Nicholson scheme for the approximation of the equations in time have been used. The resulting finite difference scheme reduces to two equations with respect to temperature and surface pressure which are solved by Richardson's iterative method. To accelerate convergence of the iterative process, filtering of the short waves is performed for the surface pressure, geopotential and zonal velocity zonal gradients in regions with  $|\phi| > \phi_{cr}$  (a value of  $\phi_{cr}$  is dependent on space resolution of the model and is equal to  $37.5^\circ$ , when  $\Delta\lambda = \Delta\phi = 5^\circ$ ). Moreover, at every time step, filtering of the waves with length equal to two steps of grid in zonal direction has been used for fields of  $u$ ,  $v$ ,  $T$ ,  $q$  and  $p_s$ .

Finally, to smooth a sharp contrast at the boundaries between ocean and continents, a correction of sensible and latent heat surface fluxes has been done by formula of type

$$\begin{aligned} \tilde{\psi}_{ij} = & \frac{1}{2} \psi_{ij} + \frac{1}{12} (\psi_{i-1,j} + \psi_{i+1,j} + \psi_{i,j-1} + \psi_{i,j+1}) + \\ & \frac{1}{24} (\psi_{i-1,j-1} + \psi_{i-1,j+1} + \psi_{i+1,j-1} + \psi_{i+1,j+1}) \end{aligned} \quad (35)$$

In (35)  $\psi$  is  $H_s$  or  $E_s$ ; the wave over a symbol refers to smoothed quantities.

Note that the described filters are single in the model and, practically, it does not change the total energy of the system. Therefore, a symmetrized form of transfer equations and the use of implicit schemes (of the Crank-Nicholson type) would in time give the possibility to construct a finite-difference scheme, which gives the exact conservation of integral quadratic invariants. Employing this method, it became possible to take off a problem of the computational instability and to do without a very strict stability criterion, replacing it with an "easier" and natural approximation criterion (Marchuk, 1974). Thus, there is a possibility to change widely in numerical experiments the coefficients in terms describing the small-scale turbulent diffusion and viscosity (practically, from zero to infinity) and to form a necessary spectral distribution of the kinetic energy.

It is necessary to note that the use of dissipation and diffusion terms in the equations for momentum and temperature exerts an influence not only on the level of the eddy kinetic energy in high wavenumber diapason but also mainly on the rate of growth or baroclinically instable modes of the synoptic scales as well. It is changing strictly the eddy transport of heat to pole and, thus, a meridional gradient of the temperature and the profile of zonal activity.

#### 4. NUMERICAL EXPERIMENTS

Let us discuss some results of three numerical experiments on the simulation of the mid-January circulation of the atmosphere. In all experiments, the temperature of the ocean's surface was assumed to be a known function of latitude and longitude and equal to climatic mid-January item.

In horizontal coordinates, the declination of the sun was fixed at mid-January too, the locations of sea-ice and continental ice were defined and the relief was absent. The following spatial resolution was used:  $5^\circ$  in latitude and longitude and three basic levels in the coordinate  $\sigma$  ( $\sigma_1 = 1/6$ ,  $\sigma_2 = 1/2$  and  $\sigma_3 = 5/6$ , which, in the absence of mountains correspond approximately to the isobaric surfaces  $p_1 \sim 150$  mb,  $p_2 \sim 500$  mb and  $p_3 \sim 850$  mb). The time step was chosen equal to 1.5 hours at stages of solving the transfer and diffusion equations and it was equal to 30 minutes at stage of adaptation. (Note that in this model a splitting-up method is used). All diabatic sources have been calculated once in 1.5 hours (except the radiative one, which was calculated once in 6 hours).

In the initial experiment (say, experiment 0), integration was carried out for 95 days from the initial state of the model atmosphere as follows:

$$u(0, \lambda, \phi, \sigma) = v(0, \lambda, \phi, \sigma) = 0 \quad (36a)$$

$$T(0, \lambda, \phi, \sigma) = T(\sigma) = 287^\circ\text{K} + 60(\sigma - 1)^\circ\text{K} \quad (36b)$$

$$q(0, \lambda, \phi, \sigma) = 0.8 q_{\max}(p_s, T(\sigma)) \quad (36c)$$

$$p_s(0, \lambda, \phi) = \text{const} = 1013 \text{ mb} \quad (36d)$$

During this integration, Arakawa's method (Arakawa, 1972) has been used to calculate the geopotential field from quasi-static equation. In further experiments (particularly those discussed below), it was useful to take for this aim a method from Corby, Gilchrist and Newson (1972).

The solution, corresponding to 95 day experiment 0 was taken as an initial state of vector  $(u, v, T, q, p_s)$  for the next three experiments I, II and III. Below, we discuss some results of these three experiments which are different only in coefficient  $\mu$  (see formula (21)). In experiment I,  $\mu = 0.1$ , in experiment II, it was equal to 1 and, in experiment III  $\mu = 10$ .

In these experiments, the integration was carried out for 90 days with the time average made for the last 30 days. It was spent about 80 sec pro one modelling day on the computer Cray-1.

In Table 1, some globally averaged characteristics for experiments I, II and III are given.

Table 1

	$K_z$	$K_E$	Z	$K_u^{tr}$	$K_v^{tr}$	$D_z^{tr}$	$D_H^{tr}$	$G^{tr}$
Experiment I	3.91	5.66	3.84	2.78	1.80	2.49	0.97	3.40
Experiment II	10.43	3.88	3.85	2.79	1.03	1.62	1.54	3.48
Experiment III	22.36	1.96	3.84	4.73	0.40	3.24	0.94	4.03

Here the following notations are used:

$K_z$  = zonal kinetic energy

$K_E$  = eddy kinetic energy

Z = absolute potential enstrophy

$K_u^{tr}$  = kinetic energy of zonal component of wind

$K_v^{tr}$  = kinetic energy of meridional component of wind

$D_z^{tr}$  = dissipation of the kinetic energy in the planetary boundary layer

$D_H^{tr}$  = dissipation of kinetic energy by subgrid-scale processes

$G^{tr}$  = generation of the kinetic energy

Units for  $K_z$ ,  $K_E$ ,  $K_u^{tr}$  and  $K_v^{tr}$  are  $10^5 \text{ J m}^{-2}$ ; units for  $D_z^{tr}$ ,  $D_H^{tr}$  and  $G^{tr}$  are  $\text{W m}^{-2}$  and units for Z are  $10^{-7} \text{ mb}^{-1} \text{ sec}^{-2}$ . The quantities  $D_H^{tr}$ ,  $D_z^{tr}$ ,  $G^{tr}$ ,  $K_u^{tr}$  and  $K_v^{tr}$  were calculated in the tropospheric layer (from Earth's surface to height equal to nearly 300 mb), the item  $K_z$ ,  $K_E$  and Z have been got by integration on whole atmosphere.

Table 1 shows that the level of eddy kinetic energy in experiment I is higher and in experiment III, it is lower than in experiment II (it is naturally); under this, a total dissipation is changed not so significantly. The "tropospheric" part of kinetic energy of zonal component of wind velocity ( $K_u^{tr}$ ) varies from experiment I to experiment III in significantly low limits than it is for total zonal kinetic energy of the model atmosphere  $K_z$ . An analysis of the temperature field at the first calculation level corresponding to the stratosphere has shown that in both experiments I and III, a new thermodynamic

regime at this level has been obtained. This new regime is warmer than in experiment II and the temperature gradient in meridional direction has a smaller zonal average. At the same time, the kinetic energy of meridional component of wind velocity varies from experiment I to experiment III in large range at all levels.

Fig. 1 presents spectra of the meridional component of kinetic energy as a function of wavenumber in experiment I (dashed line), II (solid line) and III (dashed-dotted line). One can easily see that, in experiment I, the energy transfer from synoptic scales to higher wavenumbers is considerably faster than in experiment II. At the same time, this kind of energy transfer is totally absent in experiment III. As a result, another angle of incline is obtained in experiments I and III than in experiment II. Figs. 2 - 14 illustrate the spectral distribution of eddy kinetic energy at  $45^{\circ}\text{N}$  in experiments I, II and III, respectively. Here one sees that in experiment II within wavenumbers 6 to 14, there is "-3 law" distribution. Meanwhile, the same distribution in experiment I has occurred within wavenumbers 16 to 25.

In experiment III, one can see that there is not a clearly expressed "-3 law" distribution. Though a potential enstrophy of the system does not change (an initial value of  $Z$ , corresponding to conditions (36) is equal to  $3.55 \cdot 10^{-7} \text{ mb}^{-1} \text{ sec}^{-2}$ ), however, in experiment I, an additional transport of energy to higher wavenumbers has been realised. At the same time in experiment III, a quite opposite situation has occurred. In this case, there is an additional transport of energy from synoptic scales to lower wavenumbers. Therefore, one can expect a decreasing energy exchange between zonal flow and eddies in both experiments I and III in comparison with experiment II and, of course, it must cause decreasing amplitudes of nonlinear cycles of circulation indices.

As indices of the atmospheric circulation, two characteristics have been chosen. The first index is a zonal kinetic energy  $K_z$ , the second one is an eddy kinetic energy  $K_E$ . Figs. 5 - 7 show time variations of these characteristics for experiments I, II and III, respectively.

In order to make clearer an analysis of these curves, Figs. 8 - 10 present time spectra of  $K_z$  and  $K_E$  for the last 72 days in all experiments I, II and III. One can easily see that, in experiment II, there are cycles with periods which equal approximately 14 and 24 days. It is especially noticeable for the

distribution of eddy kinetic energy. More exactly, the energy contribution of these cycles is the largest in time spectral distribution. In experiments I and III, two week and 24 day cycles are practically absent for both indices  $K_z$  and  $K_E$  and only 18 day periods have occurred in time spectral distribution of  $K_z$  in experiment I.

In conclusion, we should like to point out that excessive extension or, quite the contrary, the excessive narrowing of spatial spectrum of kinetic energy (by, in other words, a raised "turbulization" of the modelling atmosphere) might be one of the main causes of absence of the well-known "natural synoptic periods" of the atmospheric circulation.

The authors thank the administration of ECMWF for the possibility of carrying out our numerical experiments and Drs. L. Bengtsson, A. Hollingsworth and M. Tiedtke for useful discussions.

## REFERENCES

- Arakawa, A. 1972 Design of the UCLA General Circulation Model. Numerical simulation of weather and climate. Technical Report No. 7, Dept of Meteorol., University of California, Los Angeles, California. 116p.
- Blinova, E.N. 1947 About questions on mean annual distribution of the temperature in Earth's atmosphere with presence of continents and oceans (In Russian). Izvestiya (The USSR Academy of Sciences). Ser. of Geograph. and Geophys., 11, 1-15.
- Corby, G.A., A. Gilchrist, R.L. Newson 1972 A general circulation model of the atmosphere suitable for long period integrations. Q.J.Roy.Met.Soc., 98, 809-832.
- Katayama, A. 1972 A simplified scheme for computing radiative transfer in the troposphere. Tech. Rept. No. 6, Dept. of Meteorolog., University of California, Los Angeles, California, p.77.
- Kitaygorodskiy, S.A., Yu Z. Miropolskiy 1970 A contribution to the theory of active layer of open ocean (In Russian). Physics of Atmos. and Ocean, 6, No.2; 177-188.
- Kurbatkin, G.P., N.I. Lenskinov 1968 On the interaction between zonal flow and quasi-stationary ultralong wave (In Russian) Physics of Atmos. and Ocean, 4, No.6, 671-676.
- Lacis, A.A., J.E. Hansen 1974 Parameterization for the absorption of solar radiation in the Earth's atmosphere. J.Atmosci., 31, 118-133.
- Marchuk, G.I. 1958 The annual cycle of the circulation index. (In Russian). Trudy Instituta phisiki atmosphery (The USSR Academy of Sciences) No.2 114-118.
- Marchuk, G.I. 1974 Numerical solution of atmosphere and ocean dynamics problems. (In Russian). Hydrometeoizdat, Leningrad, 303p.
- McGuirk, J.P., E.R. Reiter 1976 A vacillation in atmospheric energy parameters. J.Atmosci., 33, 2079-2093.
- Miller, A.J. 1974 Periodic variation of atmospheric circulation at 14-16 days. J.Atmosci., 31, 720-728.
- Monin, A.S. 1956 On the macroturbulent exchange in the Earth's atmosphere. (In Russian). Izvestiya. (The USSR Academy of Sciences), Ser. of Geophys., No.4, 452-463.
- Rossby, C.-G. 1939 Relation between variations in the intensity of zonal circulation of the atmosphere and the displacements of the semi-permanent centers of action. J.Marine Res., 2, 38-55.
- Smagorinsky, J. 1960 On the dynamical prediction of large-scale condensation by numerical methods. Monograph No.5, American Geophysical Union, 71-78.
- Smagorinsky, J. 1963 General circulation experiments with the primitive equations: 1. The basic experiment. Mon.Wea.Rev., 91, 99-164.
- Webster, P.J., J.L. Keller 1975 Atmospheric variations: vacillations and index cycles. J.Atmosci., 32, 1283-1299.
- Wu, J. 1969 Wind stresses and surface roughness at air-sea interactions. Geoph.Rev., 74, 201-207.



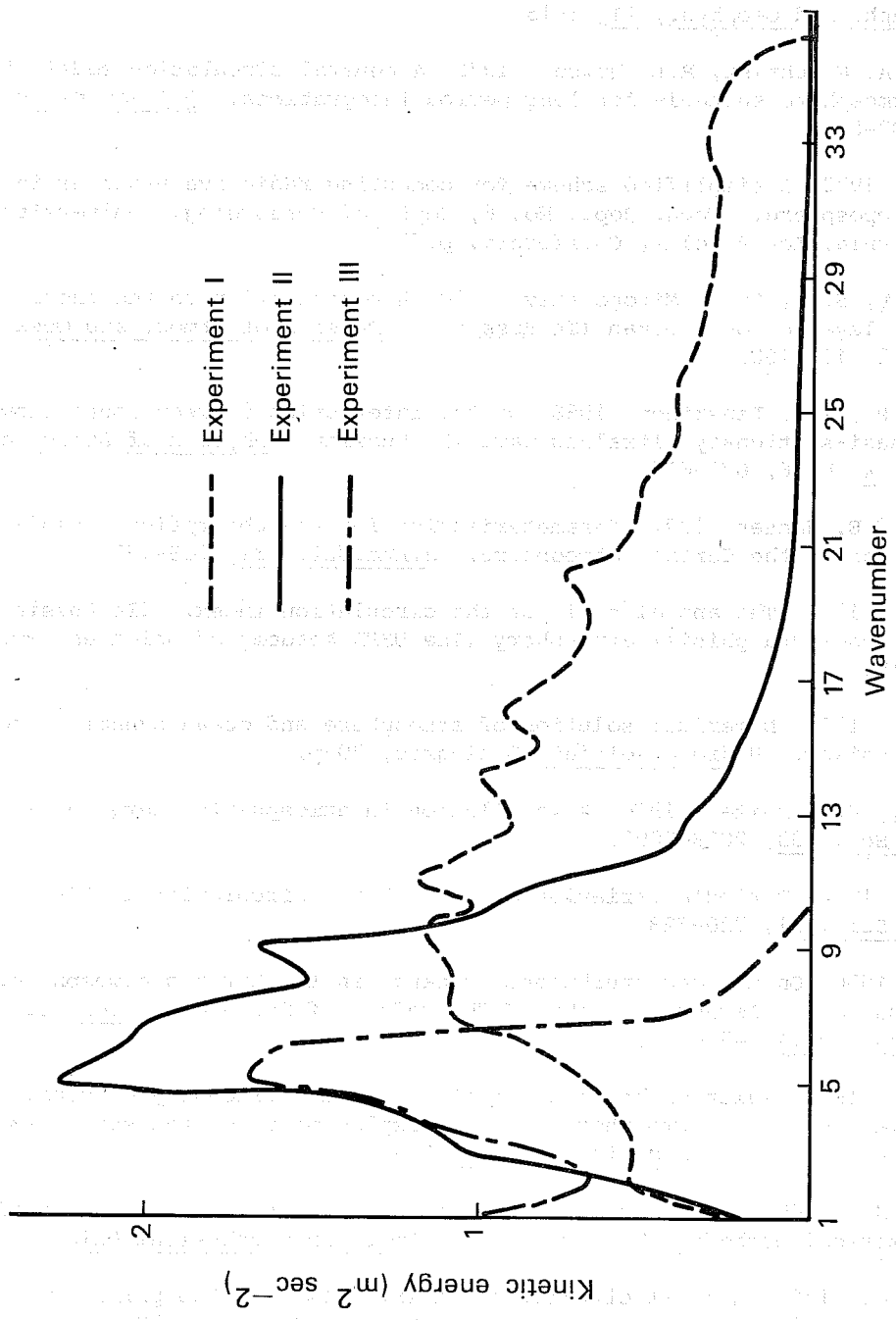


Fig. 1 Spatial spectra of meridional component of kinetic energy as a function of wavenumbers in Experiments I, II and III (dashed, solid and dashed-dotted line, respectively).

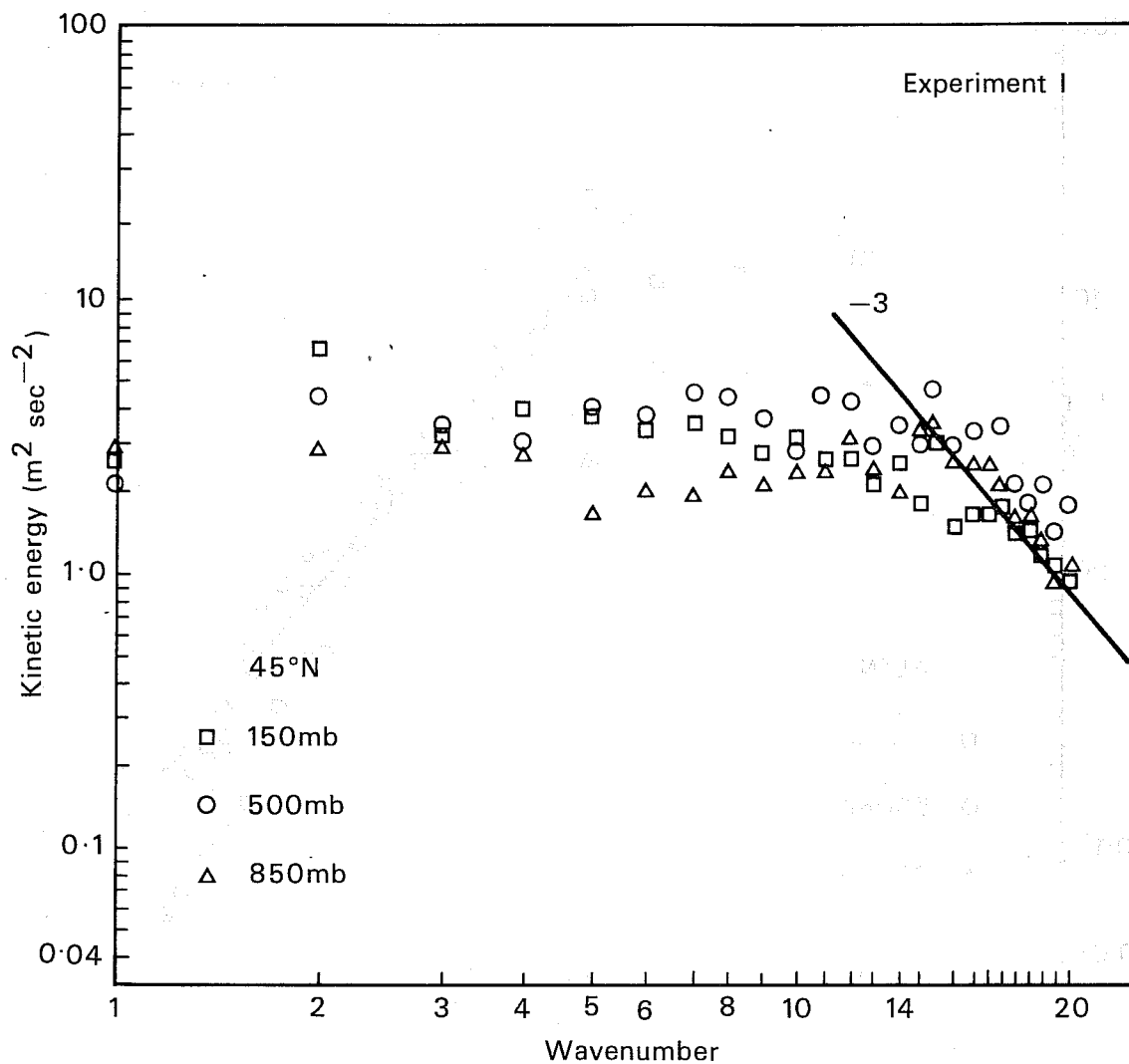


Fig. 2 Spectral distribution of eddy kinetic energy at 45°N (Experiment I).

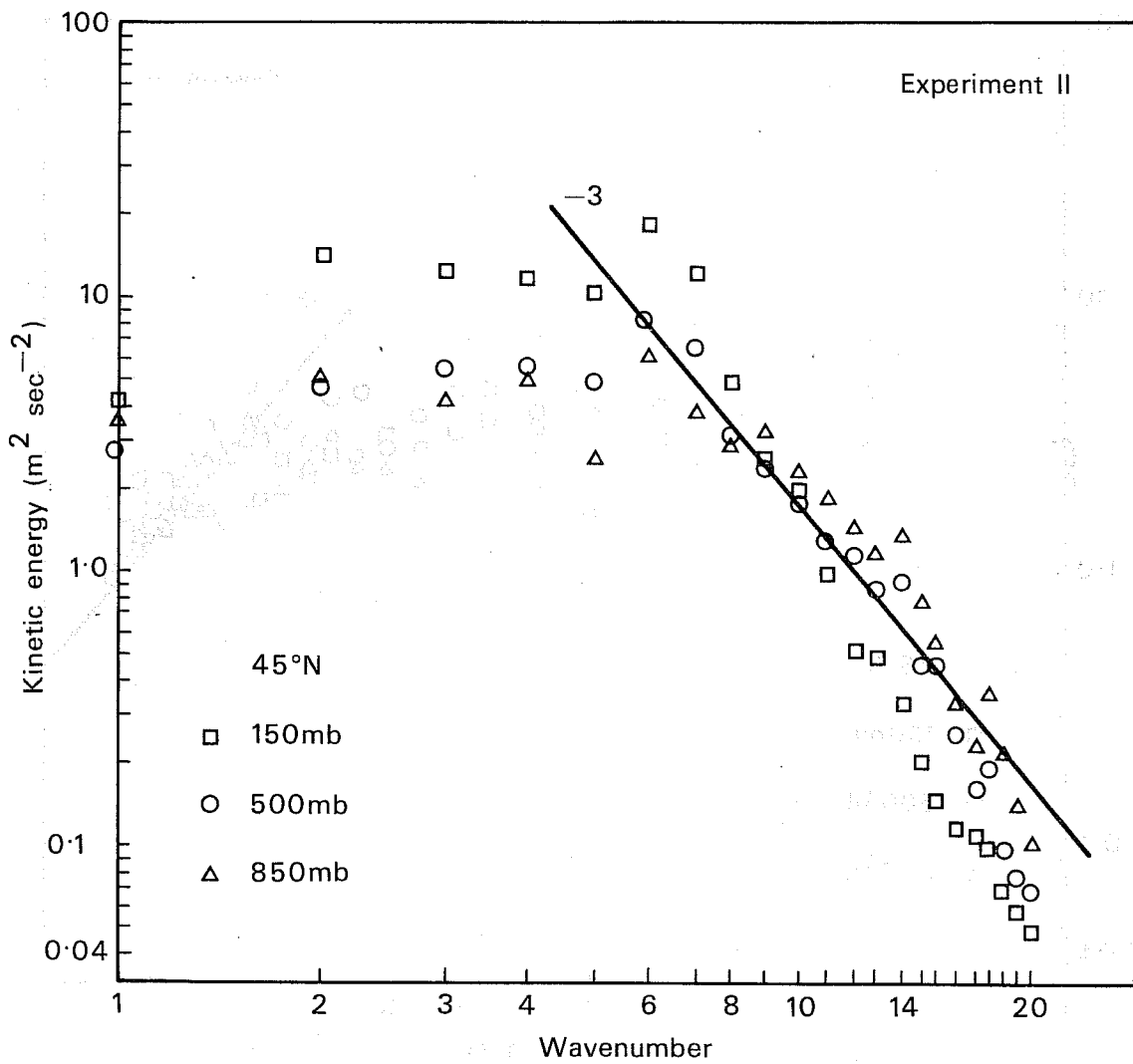


Fig. 3 Same as Fig. 2 but for Experiment II.

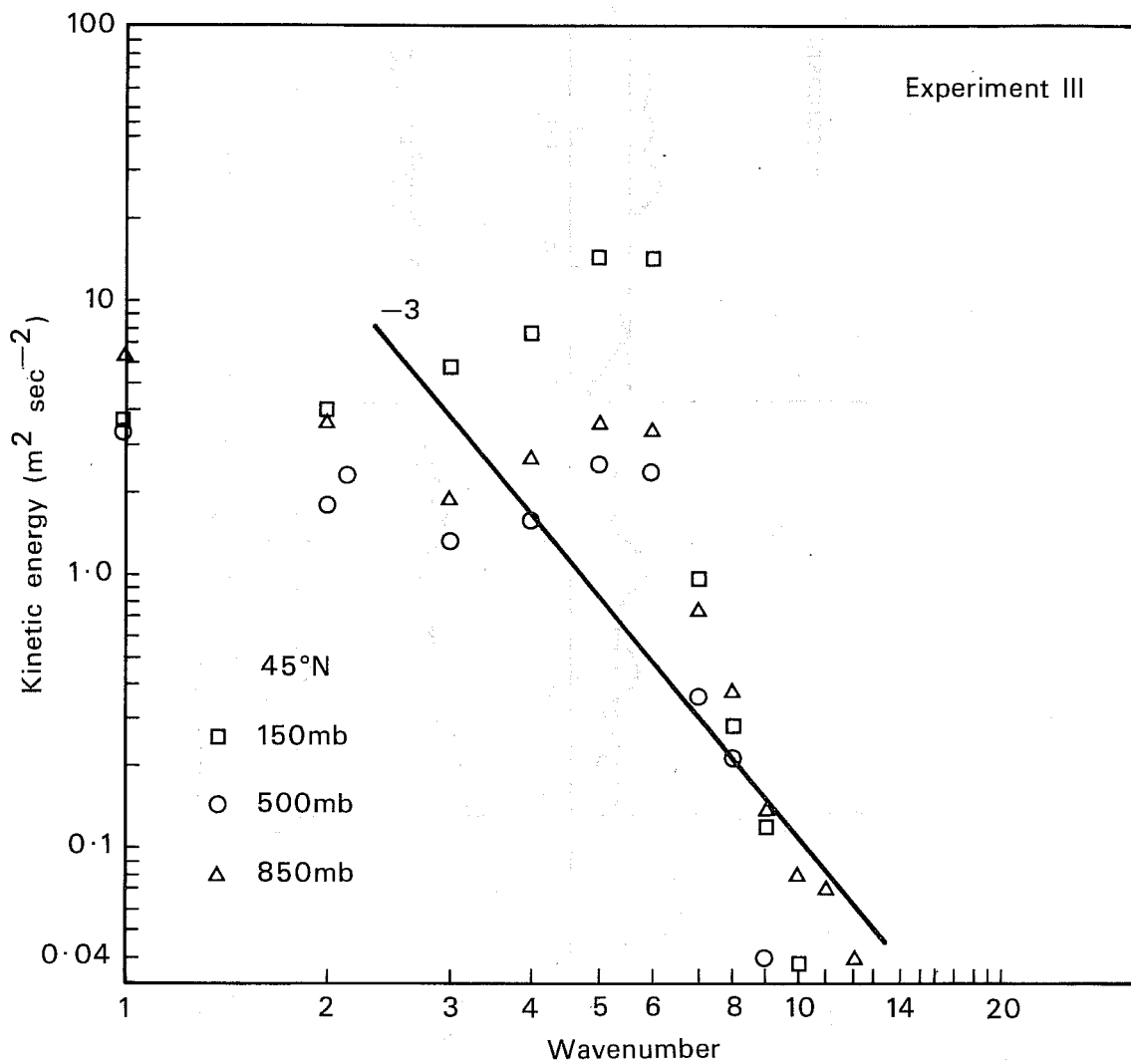


Fig. 4 Same as Fig. 2 but for Experiment III.

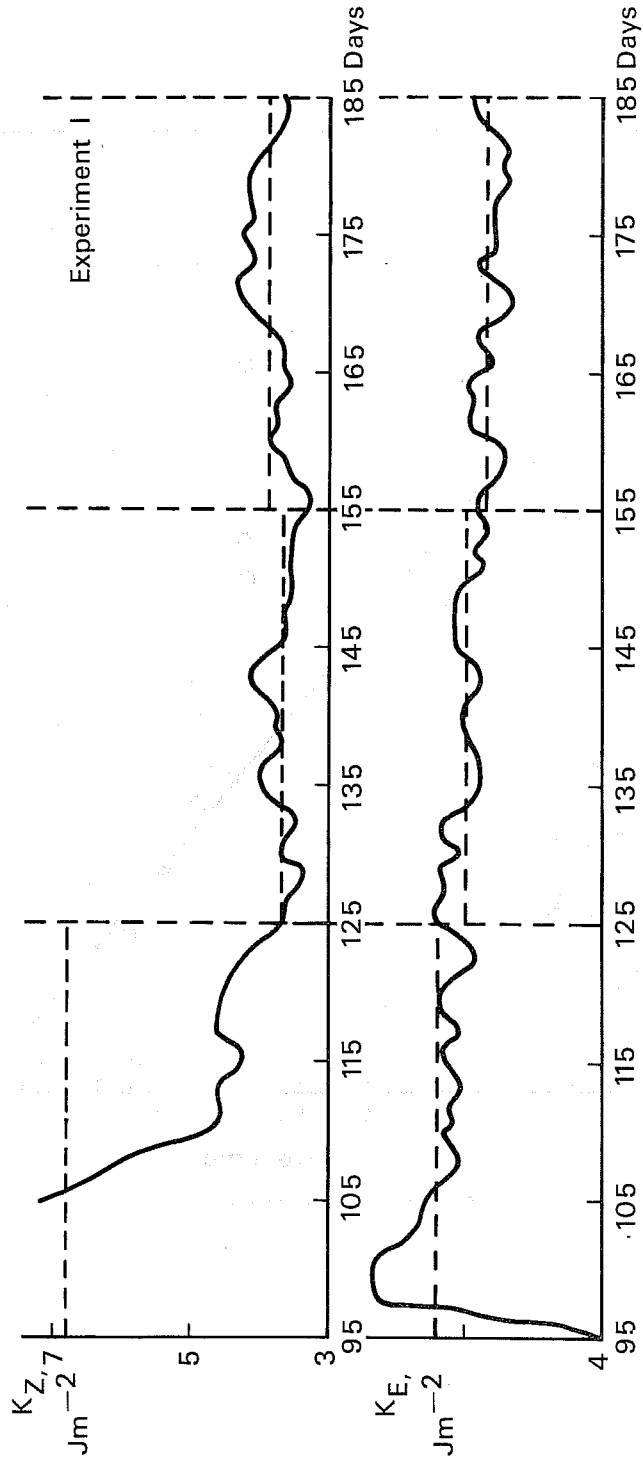


Fig. 5 Time variations of zonal kinetic energy  $K_z$  (above) and eddy kinetic energy  $K_E$  (below) for Experiment I.

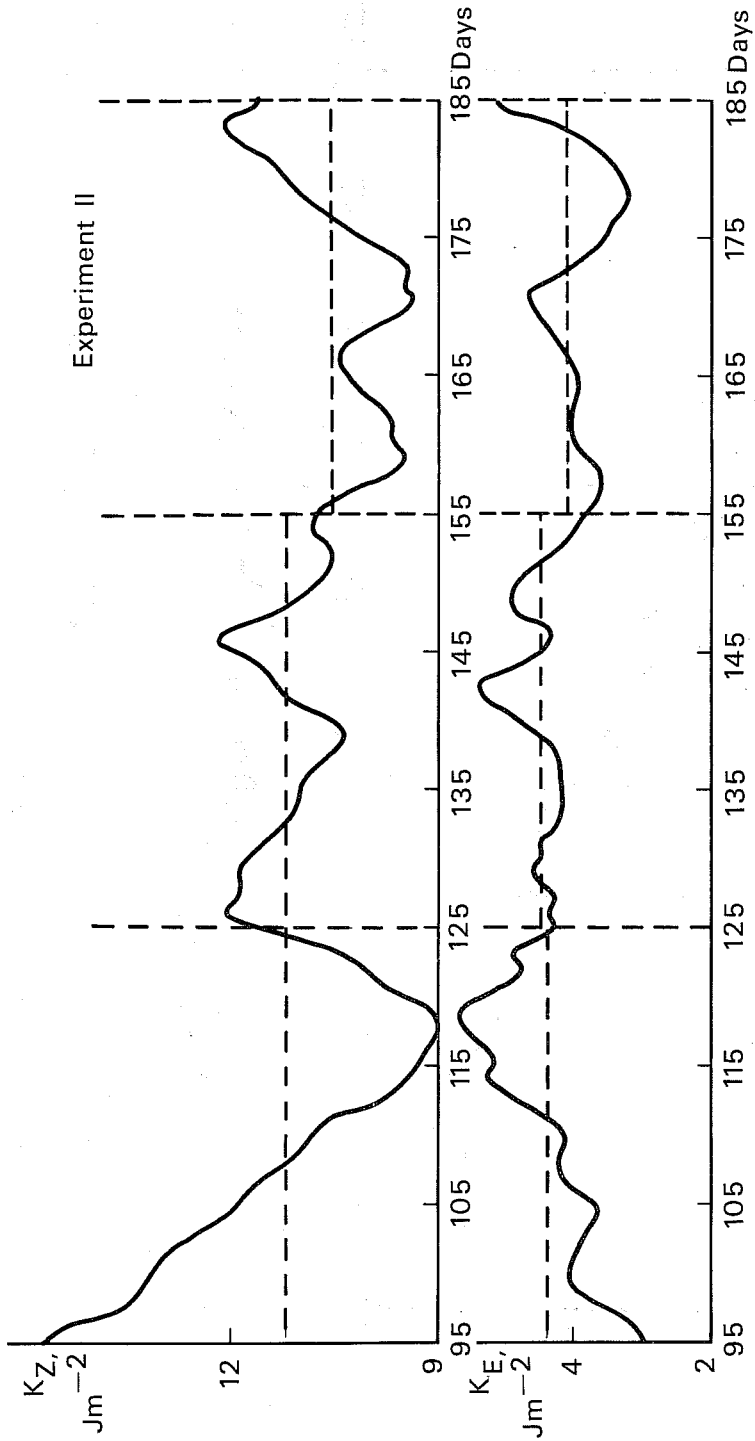


Fig. 6 Same as Fig. 5, but for Experiment II.

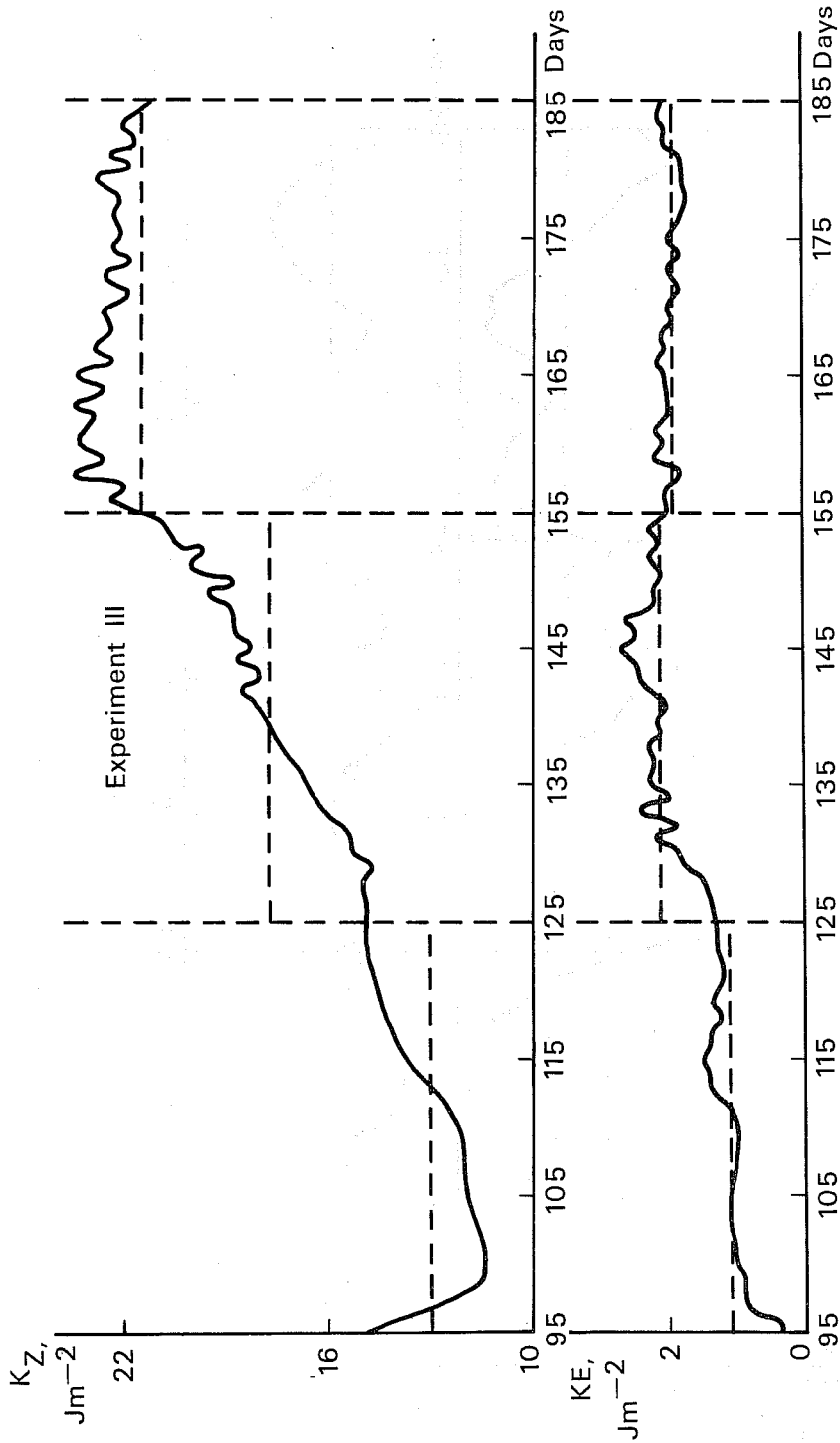


Fig. 7 Same as Fig. 5, but for Experiment III.

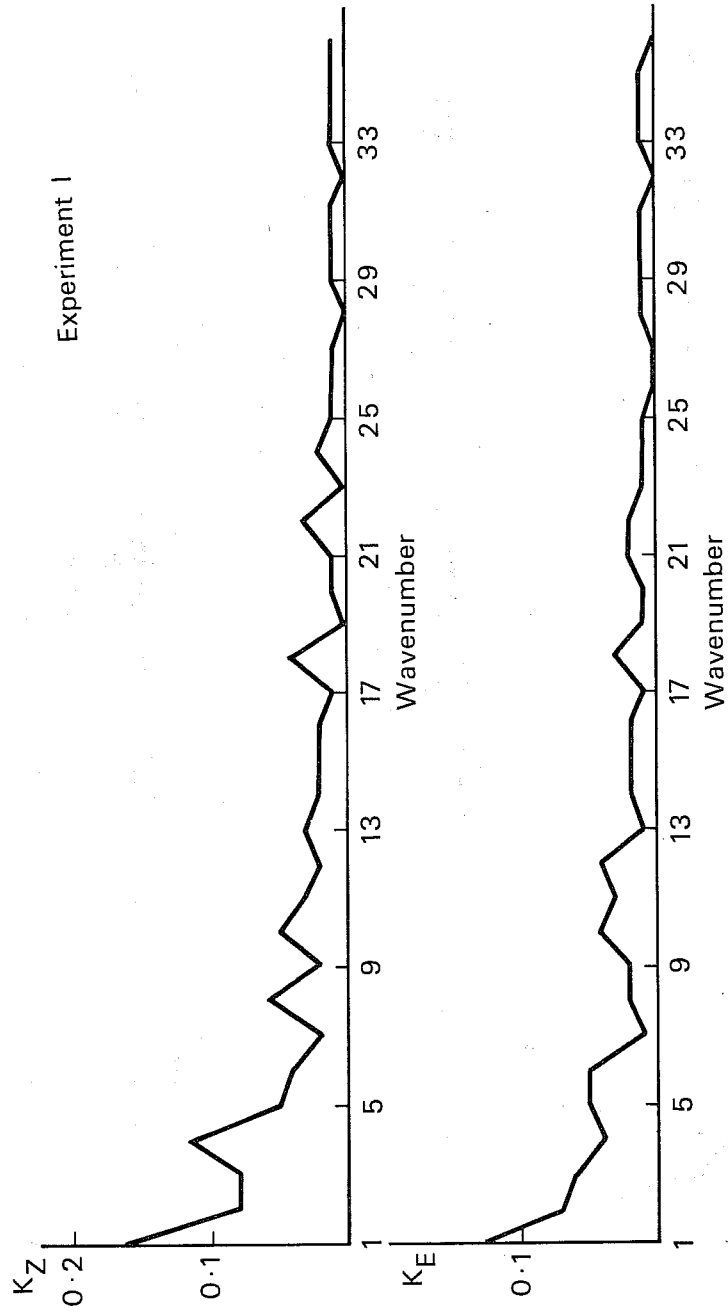


Fig. 8 Time spectra of zonal kinetic energy  $K_z$  (above) and eddy kinetic energy  $K_E$  (below) for Experiment I.



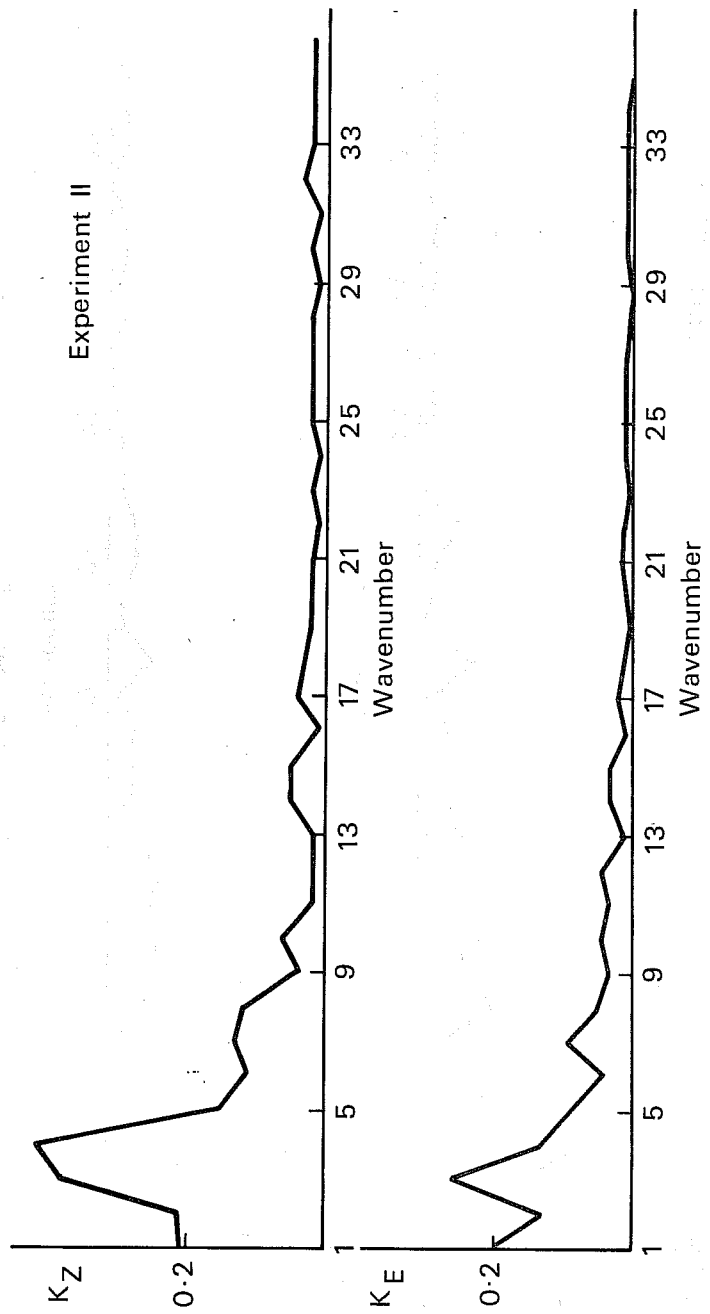


Fig. 9 Same as Fig. 8, but for Experiment II.

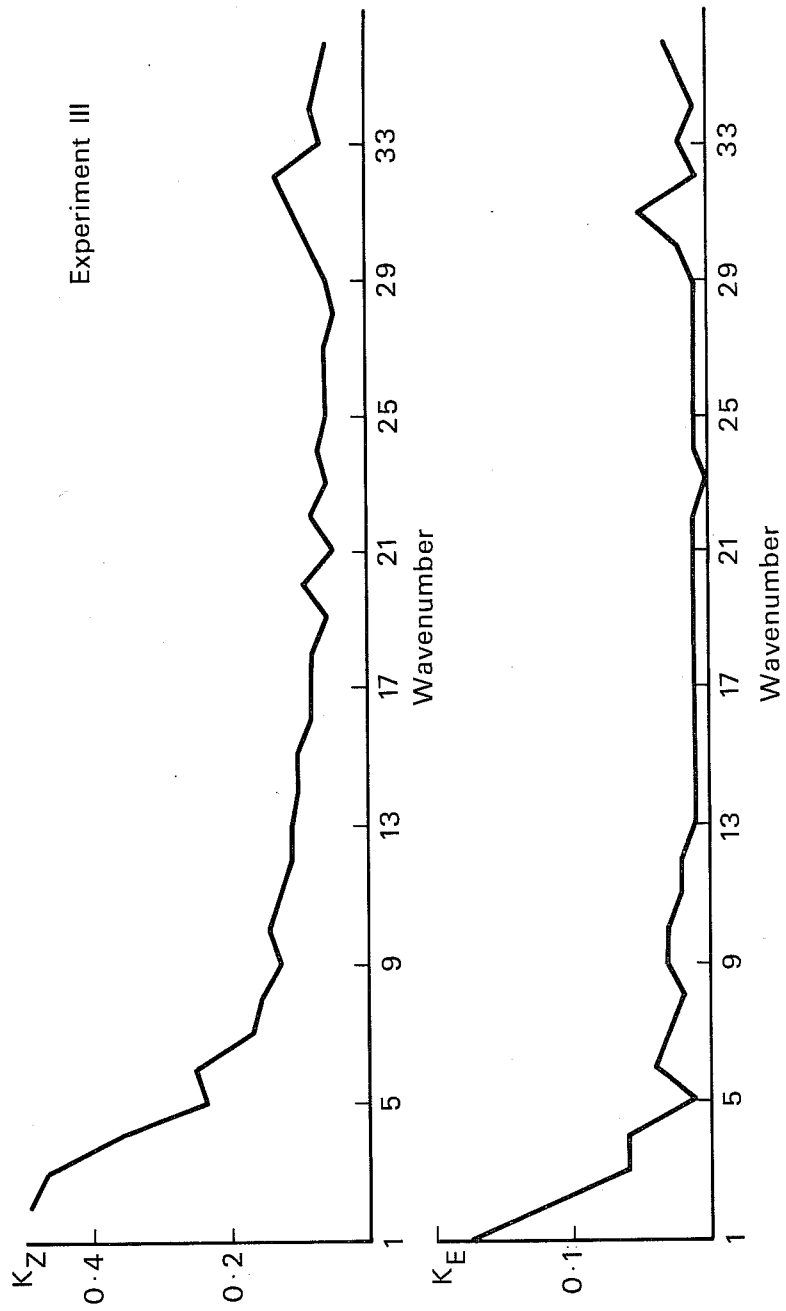


Fig. 10 Same as Fig. 8, but for Experiment III.